Journal of Alloys and Compounds 792 (2019) 529–535

Contents lists available at ScienceDirect

Journal of Alloys and Compounds

journal homepage: http://www.elsevier.com/locate/jalcom

Consolidation by MF-ERS of mechanically alloyed Al powder

E.S. Caballero [a, *], F. Ternero [a], R. Astacio [a], F.G. Cuevas [b], J.M. Montes [a], J. Cintas [a]

[a] Escuela Técnica Superior de Ingeniería, Universidad de Sevilla, Camino de los Descubrimientos s/n, 41092 Sevilla Spain
[b] Escuela Técnica Superior de Ingeniería, Universidad de Huelva, Campus El Carmen, Avda. Tres de Marzo, s/n, 21071 Huelva Spain

ARTICLE INFO

Article history:
Received 19 February 2019
Received in revised form
2 April 2019
Accepted 3 April 2019
Available online 5 April 2019

Keywords:
Mechanical alloying
Aluminium
Electrical resistance sintering
MF-ERS
FAST
ECAS
Hot pressing
Sintering
Powder metallurgy

ABSTRACT

The aim of this work is to study the viability of producing, by medium-frequency electrical resistance sintering (MF-ERS), compacts from mechanically alloyed aluminium powders. The MF-ERS process was carried out using different values of current intensity (6, 8, 10 and 11 kA) and dwelling (heating) times (400, 700 and 1000 ms). Results were compared with compacts processed by the conventional cold pressing and sintering route (850 MPa and 650 °C-1h). Depending on the processing route different properties were obtained. The final porosity of the MF-ERS compacts (23.6–7%) can be as low, under the tougher tested sintering conditions, as that of the conventionally produced compacts (6%). The compacts obtained by MF-ERS are less ductile, with lower compression strength than that obtained by the conventional route. Furthermore, a similar electrical resistance and higher microhardness can be reached by the MF-ERS process, despite the duration of the consolidation process is only a fraction of that of the conventional process.

1. Introduction

Traditionally, powder metallurgy (PM) route has consisted in two steps: cold pressing to get a green compact with the necessary strength to by handled, followed by a sintering process to obtain the final product with the required properties [1–4]. Although this method is widely used in the industrial sector, being one of its main advantages not producing waste material, other PM techniques are in a continuous development in order to achieve more environmental friendly processes. In this way, the use of electricity to consolidate powders has been experimentally approached from time ago, with the advantage of requiring just a tiny portion of the time required in traditional processing. One of the different available modes of electrical sintering [5] is known as electrical resistance sintering (ERS). This technique basically consists in applying, to a powder mass contained in an electrically insulating die, a low voltage and high intensity current and, at the same time, a low consolidation pressure [6,7]. ERS process typically lasts around one second. In such period of time, the applied voltage and pressure induce powder densification due to the heating by Joule effect. With the additional use of medium-frequency technology (developed for the resistance welding industry) it is possible to achieve lighter and smaller welding transformers, better control of current intensity and, in general, more efficient processes. The same advantages are transferred to the MF-ERS process as compared to the low frequency technology of the conventional ERS.

In the last decades, the structural applications of aluminium and its alloys have attracted much interest, mainly, in the automotive and aerospace industries [8–11]. In this way, it is interesting to achieve an improvement of their properties, either by the reinforcement with a wide variety of ceramic particles [12,13], or by grain size reduction [14,15]. Both aspects can be achieved by means of mechanical milling (MM) [16–18].

During MM, the metal powder particles are subjected to severe plastic deformation due to collisions with the various parts of the mill (walls, balls, etc.). Consequently, strong plastic deformation occurs at high strain rates (~10^3-10^4 s^{-1}) inside the particles, and the average grain size can be reduced to a few nanometres after prolonged milling. At first, MM leads to a rapid decrease in the average grain size to 40–50 nm (which constitutes a new contribution to the hardening of the material). Further refinement occurs slowly at about 15 nm after extended milling. The mean deformation at the atomic level reaches values of up to 0.7%. When the metal particles are plastically deformed, most of the mechanical

* Corresponding author.
E-mail address: esanchez3@us.es (E.S. Caballero).

https://doi.org/10.1016/j.jallcom.2019.04.024
0925-8388/

energy spent in the deformation process is converted into heat, but the rest is stored in the metal, in the form of dislocations and other defects that strongly harden the metal. The effect of adding reinforcing ceramic particles, and even the size of these reinforcing particles, clearly affects the evolution and final characteristic of the milled powder [19]. On the other hand, when more than one base material is considered, the process can evolve in a much more complicated way, for instance with the presence of amorphous layers surrounding nanocrystals of a particular composition, and the subsequent crystallization of the amorphous phase for longer milling times [20].

MM was first investigated in detail for a series of high melting temperature metals with bcc and hcp crystalline structures. Metals with fcc structure are inherently more ductile and often show a stronger tendency to adhere to container walls and balls and weld to larger particles, often several millimetres in diameter, during the milling process. To avoid this, a process control agent (PCA) is added, essential to avoid excess soldering and guarantee the subsequent refining of the grain. Thus, even though the milling process is carried out with a pure powder, carbon, oxygen and nitrogen atoms from the PCA are incorporated in solid solution hardening the material, and could originate dispersed particles during the sintering process.

The improvements made to the powder would be of little interest if they did not survive the consolidation process. Often, the high temperature exposure during sintering degrades the improvements made to the powder, e.g., increasing grain or dispersoids size. The choice of sintering conditions is therefore not an easy task. It is here that the extraordinary speed of electrical consolidation techniques can play an important role, reducing high temperature exposure to seconds, compared to 30–60 min for conventional sintering.

In the present work, MF-ERS technique has been used to prepare compacts from aluminium powder milled for 5 h in vacuum. After consolidation, compacts densification was measured, and microstructural studies were carried out. Likewise, microhardness, electrical resistivity and compression strength were determined, and results were compared with those obtained following the conventional consolidation route.

2. Materials and experimental procedure

As starting material, as-received elemental aluminium powder (AS 61, Eckart, Germany) was used. The powder was mechanically alloyed for 5 h in vacuum. A 3 wt% of ethylene bis-stearamide (EBS) micropowder organic wax was used as PCA to control the balance between the welding and fracture processes of the Al powder during milling. The 1400 cm^3 water-cooled stainless steel vessel was filled with 72 g of powder and 3600 g of balls (charge ratio in wt.%: 50:1). Milling process allows reducing Al particle size from D [4,3] of 80.5 μm to 29 μm (Fig. 1), as well as incorporating into the powder particles both the superficial aluminium oxide (Al_2O_3) layers and the carbon coming from the wax used as PCA.

Milled powder were submitted to a degassing process consisting in a vacuum (5 Pa) heat treatment at 350 °C for 30 min, followed by furnace cooling. This is a necessary process to avoid that, during the heating stage of the MF-ERS process, gasses can be released once the powders form a material with closed porosity, therefore avoiding the material densification. Experiences carried out directly with as-milled powders reach a low densification, even lower for higher intensity and heating times, which are the proper conditions for both quickly reach a closed porosity and releasing a higher amount of gases.

The consolidation process using MF-ERS was carried out in a medium-frequency resistance welding machine (Serra Soldadura, S.A., Spain) appropriately adapted for this purpose. The consolidation pressure was 100 MPa for all the experiences, in an alumina die wall–lubricated with graphite, and a powder mass of 1.8 g that were initially vibrated up to reach their tap density [21]. Different current intensities (6, 8, 10 and 11 kA) and dwelling (heating) times (400, 700 and 1000 ms) were employed to test the influence of these parameters on the powder consolidation. Final specimens attained 12 mm in diameter, according to the die inner orifice, and heights between 5.5 and 6.5 mm, depending on the consolidation conditions.

MF-ERS experiments start with a *cold-pressing period* (lasting 1000 ms) under constant pressure and no current passing through the powder. Then, electrical current is applied in the *heating and pressing period*. The consolidation finishes by only applying pressure for 300 ms during the *cooling/forging period*.

For comparative purposes, cylindrical compacts of 1.8 g were also produced following the conventional PM route of cold pressing and furnace sintering. Milled powders were vibrated to reach their tap density and uniaxially cold pressed at 850 MPa in a hardened steel die 12 mm in diameter, and sintered in vacuum (5 Pa) at 650 °C for 1 h.

Powders morphology was observed by scanning electron microscope (SEM, FEI TENEO), while an optical microscope (Nikon Epiphot 200) was used for microstructural studies. Crystallite size and microstrain of the phases formed during sintering were calculated by the Le Bail method [22] on X-ray diffraction patterns (XRD, Bruker D8 Advance, using CuKα radiation). Because of the compacts symmetry, Vickers Microhardness HV1 (Struers DURAMIN-A300) was only measured in one quadrant (Fig. 2) of a longitudinal section of the samples.

For the electrical resistance measurements at room temperature, a four points probe and a Kelvin bridge with a measuring range between 0.01 μΩ and 1000 Ω were used. The thermoelectric effects were eliminated by changing the probes polarity in the measurements, and the mean value was considered for each

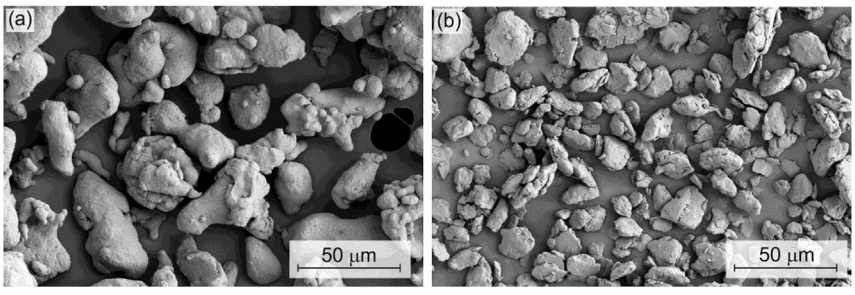

Fig. 1. SEM micrographs of (a) as-received and (b) milled aluminium powder.

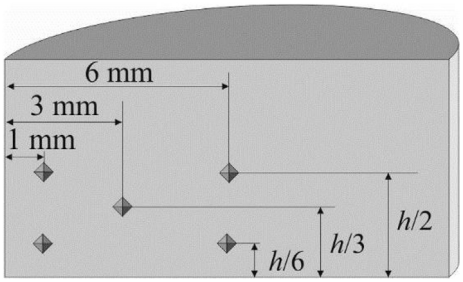

Fig. 2. Diametrical section of cylindrical compacts with the distribution of hardness points.

specimen. Compression tests were performed in a universal testing machine (Instron 5505), up to compacts breaking or until achieving a strain of 50%, whatever happens first.

3. Results and discussion

The viability of applying the MF-ERS process to MM Al powder has been first analysed according to the porosity reached, although a detailed analysis of the different areas of the compact has been carried out because of the non-homogeneous structure typical of electrical consolidation processes. Once known the microstructure, the actual degree of sintering, i.e., whether particles really show metal-metal contacts has been checked by measuring both the microhardness of the prepared materials and their electrical resistivity, both properties very much related to the microstructural characteristics of the material. Finally, the macroscopic behaviour of the compacts was analysed by studying their compression behaviour.

3.1. Final porosities

Final porosities for all the compacts were determined from their final dimensions, once determined the absolute density of the powder by picnometry, with a value of 2.56 g/cm^3. The final porosity of the different compacts obtained by MF-ERS is shown in Table 1 as a function of the current intensity (I) and the heating time (t). As expected, porosities decrease for higher current intensities and heating times. Thus, it would be possible to estimate the final porosity of compacts, from the sintering parameters (I, t).

On the other hand, compacts prepared by the conventional PM route (pressing and sintering) achieved a porosity of 6.5% after the pressing step, which is reduced down to 6% after being sintered. It is remarkable that the porosity in compacts obtained by MF-ERS can be relatively closer to that achieved for compacts produced by the conventional route, even though pressing and sintering times are very different. Conventional route needs pressing and a sintering stages, in general, lasting more than 1/2 h. On the contrary, the whole MF-ERS process lasts less than 1 s.

Table 1
Values of the compacts final porosities (Θ_F) in %, for the different MF-ERS experiments.

		Heating time [ms]		
		400	700	1000
Intensity [kA]	6	23.6	20.0	17.6
	8	19.0	14.3	12.5
	10	15.2	12.5	10.5
	11	12.3	11.1	7.0

3.2. Microstructural study

A microstructural study was carried out in order to evaluate the porosity distribution obtained for both methods. As can be seen in Fig. 3, a spherical, small and uniformly distributed porosity is present in the sample obtained by the conventional route.

However, the porosity distribution in MF-ERS compacts is non-uniform (Fig. 4). The lack of uniformity is mainly due to a non-homogeneous temperature distribution during the MF-ERS process. As observed by Lenel [23], temperature is higher in the centre, and lower in the bases and sides of the compact. As shown in diametrical section of Fig. 4, the periphery is more porous than the centre (darker in the images).

Figs. 5 and 6 show detailed micrographs of the inner structure of MF-ERS compacts, the first in the corner of the compact and the second in the section centre. Both sets of images clearly show that the porosity degree deceases for tougher electrical consolidation conditions (higher current intensities and/or heating times).

According to the micrographs, the intensity seems to be some more determining than the heating time with regard to the obtained porosity. Only with 10 or 11 kA the corner of the compact acquires a relatively low porosity, being quite dense for 11 kA−1000 ms. The centre, however, reaches a low porosity for any of the compacts prepared with 10 or 11 kA and even for 8 kA−1000 ms.

On the other hand, the Al grain size and microstrain attained after consolidation has been calculated by the Le Bail method [22] applied to the XRD patterns. Representative results in Table 2 show that bigger grain size and lower microstrain are attained after conventional consolidation, with grain size of approximately 140 nm. MF-ERS compacts reach grain sizes in the order of 65−90 nm depending on the consolidation conditions.

Results can be explained because of the longer time at higher temperature of compacts processed by the conventional route, this makes Al grain size to grow and microstrain to decrease. Al_4C_3 grains appearing because of the wax used as PCA in the MM process result however with a very similar grain size for the different sintering conditions. This phase appears as independent grains [24] in the Al matrix with no option to grow because of tougher heat treatments.

It is also worth noting that only Al and Al_4C_3 can be detected in

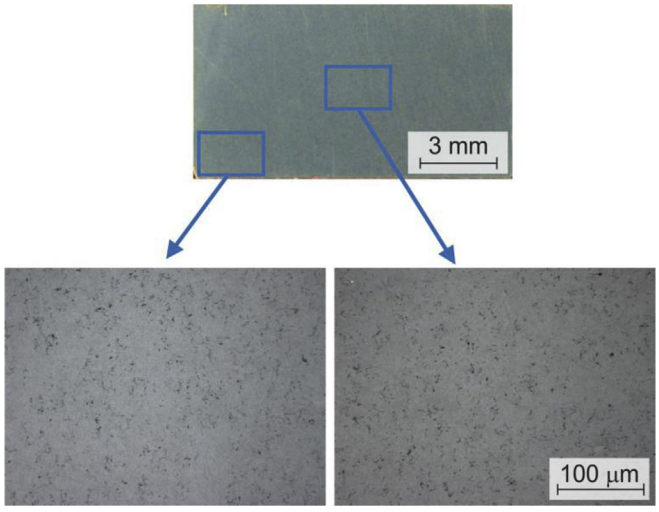

Fig. 3. Porosity distribution of a diametrical section of a conventionally consolidated compact: macrograph of the whole section (top) and micrographs at the corner and centre (bottom).

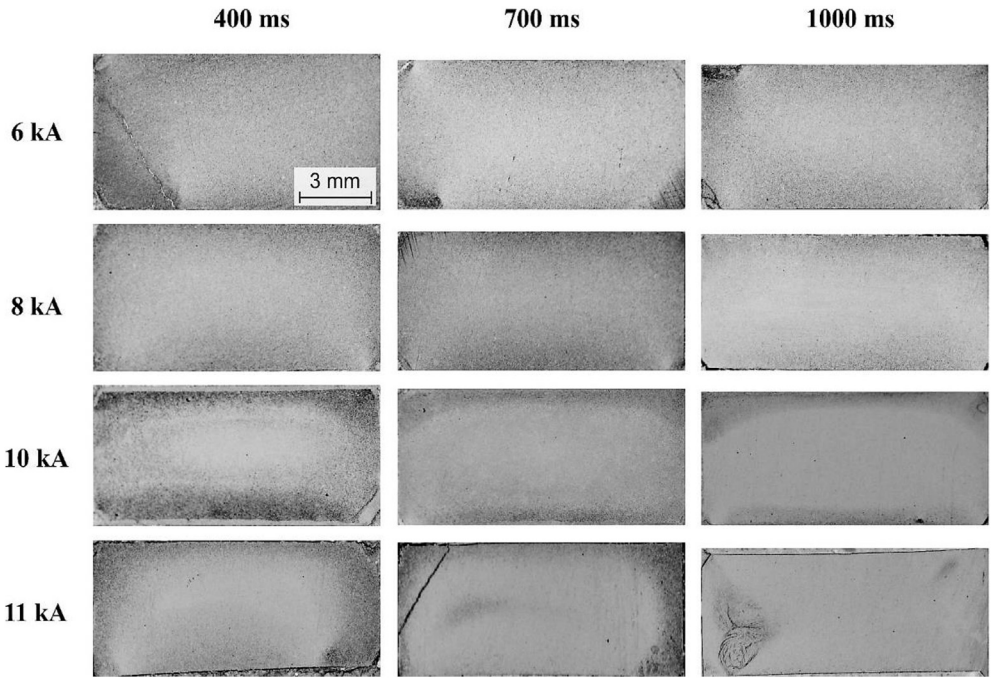

Fig. 4. Porosity distribution in MF-ERS Al compacts. Lighter areas (more reflecting) indicate a lower porosity content (higher densification).

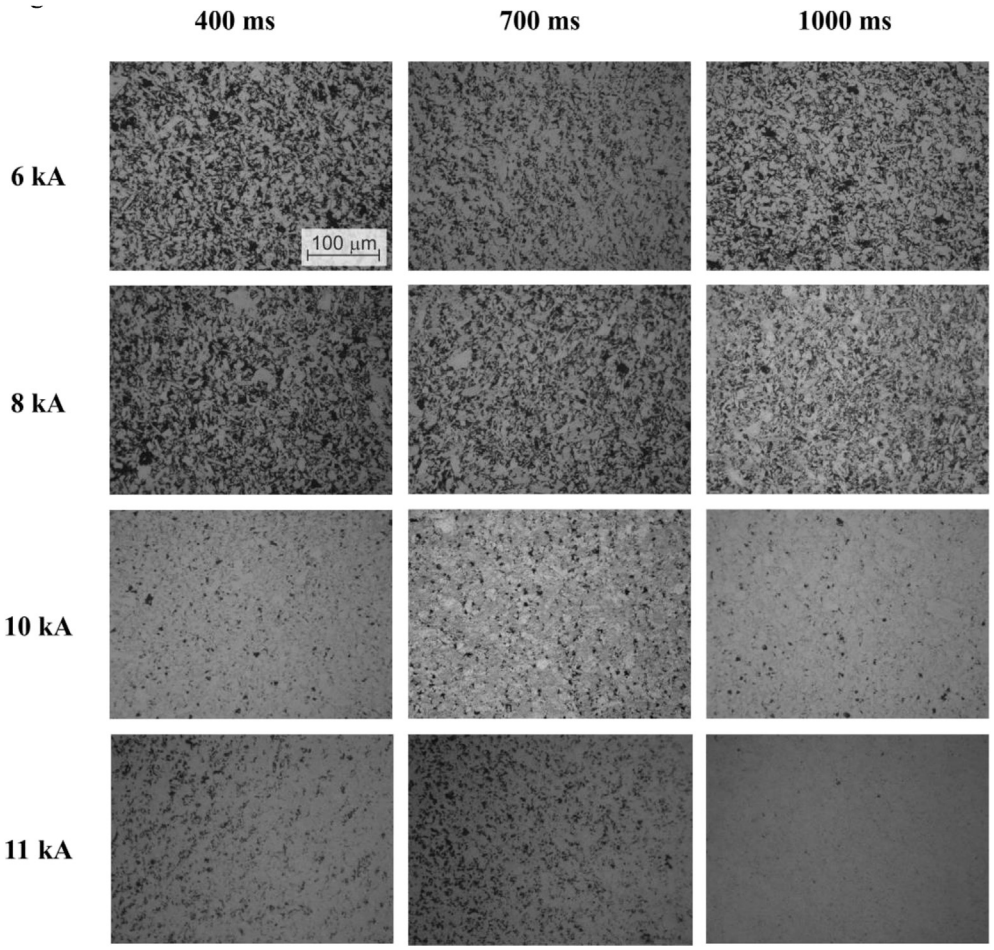

Fig. 5. Micrographs showing the porosity distribution in a corner of diametrical sections of MF-ERS compacts consolidated under different conditions.

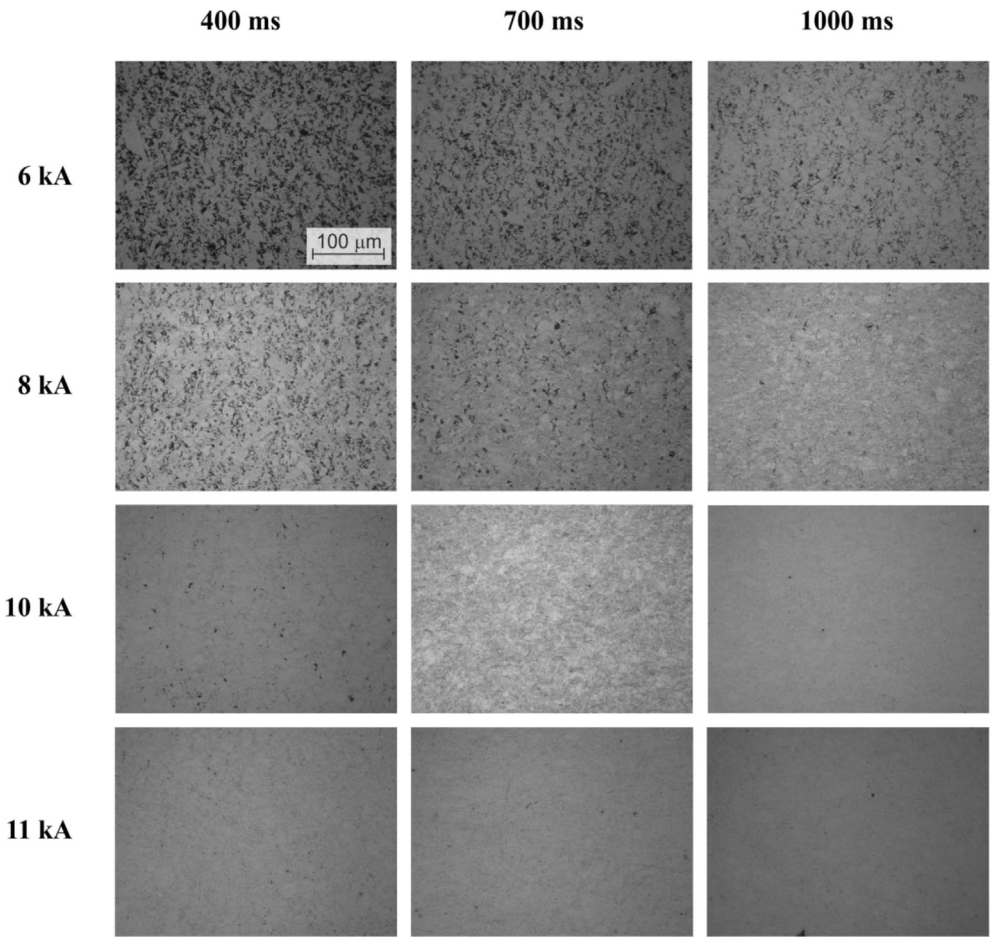

Fig. 6. Micrographs showing the porosity distribution at the centre of diametrical sections of MF-ERS compacts consolidated under different conditions.

Table 2
Al and Al_4C_3 grain size and microstrain for conventional compacts and representative MF-ERS experiments. R_{wp}, regarding the goodness of the fitting process, is shown.

		Al		Al_4C_3		R_{wp}
		Grain size (nm)	Microstrain	Grain size (nm)	Microstrain	
Conventional		139.0	0.000393	29.1	0.00008	6.15
MF-ERS [kA-ms]	6–400	66.1	0.000819	31.9	0.00040	5.06
	8–700	79.5	0.000765	32.8	0.00035	5.36
	10–700	89.7	0.000735	31.4	0.00030	5.61
	11–1000	92.3	0.000678	33.2	0.00037	5.49

these detailed XRD patterns, resulting a proportion of approximately 90.3 and 9.7% for any of the studied compacts. This means that the amount of alumina coming from the surface of the original particles is very low. Although the presence of oxides in native metallic particles for sure affects the electrical properties, this is not the case regarding mechanical or electrical properties in MM Al powder. The oxide layer in Al powders is only a few nanometres width [25,26], and once powders are MM and oxide from the particles surface is incorporated inside the particles, its presence is small enough to make very little effect on measured properties, whichever the conventional or electrical processing applied.

3.3. Microhardness distribution

Mean microhardness of a conventionally consolidated compact, after measuring in the five point of Fig. 2, resulted 102 ± 2 HV1. On the other hand, Table 3 gathers the mean values and standard deviation from the five tested points, for the MF-ERS specimens. Because of the non-uniform distribution of the porosity, consequence of the different temperatures reached on different zones of the compact, hardness also shows a clear non-uniformity inside the compacts.

Table 3
Mean values and standard deviations of microhardness (HV1) for the different MF-ERS experiments.

		Heating time [ms]		
		400	700	1000
Intensity [kA]	6	72 ± 21	85 ± 14	98 ± 26
	8	74 ± 20	111 ± 32	113 ± 31
	10	112 ± 39	123 ± 53	114 ± 50
	11	124 ± 43	135 ± 40	168 ± 3

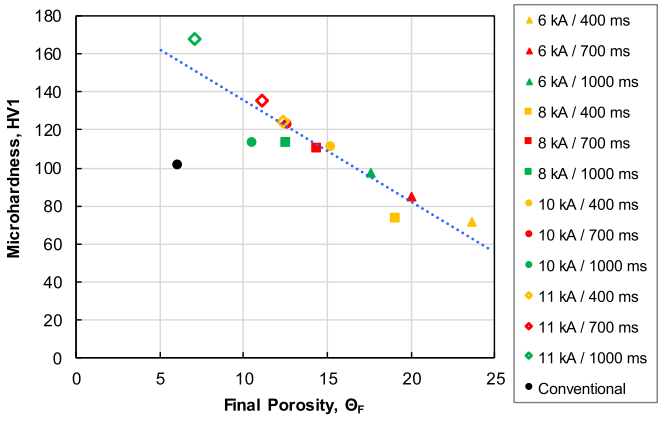

Fig. 7. Mean microhardness (HV1) vs. final porosity of the compacts for the different MF-ERS compacts and the conventional compact.

Mean microhardness of MF-ERS specimens consolidated under the more severe conditions reaches values higher than that of the conventional compacts. Nevertheless, the standard deviations take very high values (up to 53, versus 2 for conventional processing). This represents an image of the non-uniform microstructural level typical of electrical consolidated compacts.

Fig. 7 represents the microhardness vs. porosity for the different compacts. Values show an approximately linear correlation, demonstrating the well-known strong dependence of the microhardness on the porosity. Nevertheless, it is worth noting that the hardness value of the conventional compact does not correspond to the expected value in the trend line of the data corresponding to the MF-ERS compacts. This shows the big difference between the conventional and electrical processes. The very short MF-ERS process makes the powder to maintain both a small grain size and a high hardness attained after mechanical milling, with the relatively low temperature of the degassing process not being enough to soften the powder. However, the conventional process, with exposure to higher temperatures, makes the powder increase Al grain size up to about twice that of MF-ERS compacts and decrease microstrain to the half, therefore the conventional compact showing a lower microhardness.

3.4. Electrical resistivity

The electrical resistivity is a property very much sensible to the microstructural characteristics of the materials. It is especially sensible to the presence of porosity characteristic of PM materials. Moreover, in these materials, the resistivity typically depends on the goodness of the metal-metal contacts among particles, because of the presence of oxide layers surrounding the metallic powder particles. Alumina (the natural oxide of aluminium) is especially resistant, both mechanically and electrically, thus its presence is much influencing. However, once powders are MM and the alumina layer incorporated to the powder particles, its influence is negligible. Table 4 gathers the measured electrical resistivity values for all the MF-ERS compacts.

These values must be compared with the value of the specimen conventionally consolidated conventionally, whose value was $7.38 \cdot 10^{-8}\,\Omega\,m$. As shown in Fig. 8, this value is some lower than those obtained with the tougher electrical consolidation conditions, although is in the expected trend with regard to the porosity values. This allows concluding that the value is a consequence of the lower porosity and not of cleaner metal-metal contacts. This is a logical conclusion for the studied materials, which were milled previously to the consolidation process.

Table 4
Values of electrical resistivity (expressed in $\Omega \cdot m$) for the different MF-ERS compacts.

		Heating time [ms]		
		400	700	1000
Intensity [kA]	6	$15.0 \cdot 10^{-7}$	$10.1 \cdot 10^{-7}$	$9.74 \cdot 10^{-7}$
	8	$7.71 \cdot 10^{-7}$	$6.11 \cdot 10^{-7}$	$5.59 \cdot 10^{-7}$
	10	$4.49 \cdot 10^{-7}$	$4.04 \cdot 10^{-7}$	$3.00 \cdot 10^{-7}$
	11	$4.22 \cdot 10^{-7}$	$2.51 \cdot 10^{-7}$	$1.51 \cdot 10^{-7}$

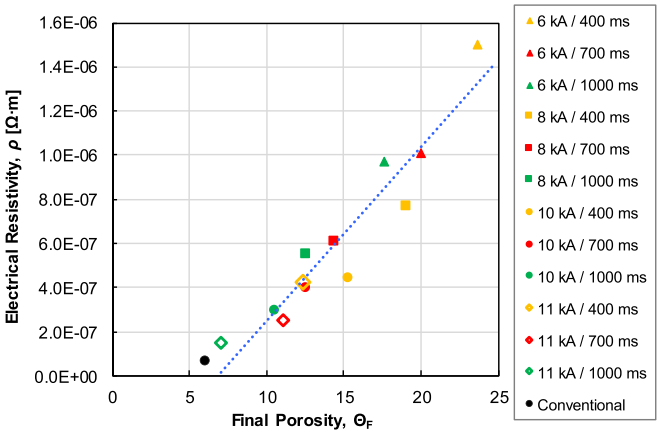

Fig. 8. Electrical resistivity vs. final porosity for the MF-ERS compacts and the conventional compact.

3.5. Compression tests

Concerning the compression strength, values achieved by MF-ERS are between 181 and 420 MPa, as shown in Table 5. Higher compression strengths are attained for higher values of intensity or heating time, because of the better sintering process. However, the low porosity achieved by the conventional route, as result of applying a much higher pressure and longer sintering times, allows achieving strengths as high as 600 MPa (after a strain of 50%), mainly as a result of the bigger grain size and better ductility achieved after the prolonged heat treatment that supposes the furnace sintering process.

Fig. 9 compares the values of Table 5 and the value of the conventional compact. The influence of the porosity degree is again the prominent parameter among the MF-ERS materials, showing a linear trend. However, the conventional compact does not follow the trend of the electrically consolidated specimens, again showing the significant difference between both processes, and the effect of the bigger grain size and long exposure to high temperature of the conventionally consolidated compact. According to this, the conventional compact shows a more ductile behaviour, with a higher value of compression strength because of making possible reaching

Table 5
Values of compression strength (expressed in MPa) for the different MF-ERS compacts.

		Heating time [ms]		
		400	700	1000
Intensity [kA]	6	181	228	222
	8	224	258	266
	10	276	341	376
	11	299	380	420

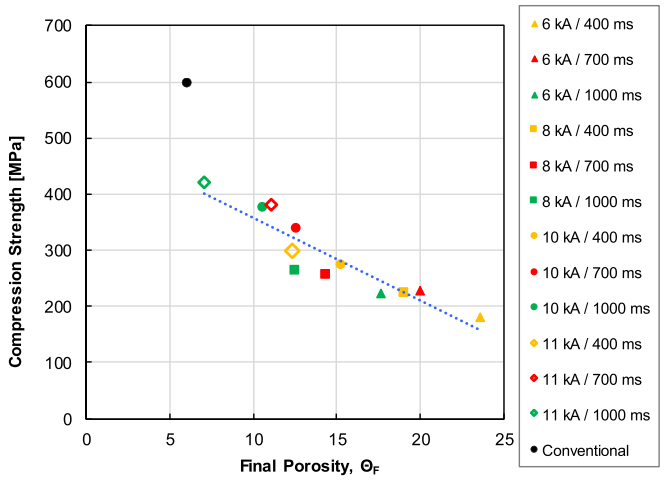

Fig. 9. Compression strength versus porosity of the compacts obtained by MF-ERS.

the upper strain limit of 50%, something not possible in MF-ERSed specimens, which break at about 10–20% strain depending on the electrical sintering conditions.

4. Conclusions

Compacts of mechanically milled Al powders consolidated by the MF-ERS technique, using different current intensities (6, 8, 10 and 11 kA) and dwelling times (400, 700 and 1000 ms), have been produced. This technique has been proved to correctly consolidate Al hardened powders. Results show that the final porosity clearly depends on the current intensity, with a lower dependence on the heating time. According to the microstructure, only 10 and 11 kA produce compacts with low enough porosity, nevertheless being slightly higher in the compact periphery. Compacts prepared according to the conventional PM route achieve as low porosity as that obtained by MF-ERS under the most severe conditions (highest intensity and time). According to the porosity of the different compacts, the microhardness of the MF-ERS compacts is higher than expected when compared with the conventionally consolidated specimen. However, the compression strength is lower. The high hardness attained in the powders after milling is maintained in MF-ERS compacts because of the very short exposure at high temperatures, nevertheless, the long exposition to temperatures of conventionally consolidated compacts results in a better particles joining and more ductile materials. Regarding the electrical resistivity, both processes behave with the expected trend, showing that the descaling of the oxide layer and the metal-metal contacts are similar in both consolidation processes.

Acknowledgement

Financial support of the Ministerio de Economía y Competitividad (Spain) and FEDER (EU) through Research Projects DPI2015-69550-C2-1-P and DPI2015-69550-C2-2-P is gratefully acknowledged.

References

[1] F. Fitriani, S.M. Said, S. Rozali, M.F.M. Salleh, M.F.M. Sabri, D.L. Bui, T. Nakayama, O. Raihan, M.M.I. Megat Hasnan, M.B.A. Bashir, F. Kamal, Enhancement of thermoelectric properties in cold pressed nickel doped bismuth sulfide compounds, Electron. Mater. Lett. 14 (2018) 689–699.
[2] F.G. Cuevas, J. Cintas, J.M. Montes, J.M. Gallardo, Al-Ti powder produced through mechanical alloying for different times, J. Mater. Sci. 41 (24) (2006) 8339–8346.
[3] E.S. Caballero, F.G. Cuevas, F. Ternero, R. Astacio, J.M. Montes, J. Cintas, In situ synthesis of Al-based MMCs reinforced with AlN by mechanical alloying under NH_3 gas, Materials 11 (5) (2018) 1–9.
[4] F. Safari, R. Azari Khosroshahi, A. Zokriasatein, Wear behavior of copper matrix composites reinforced by γ-Cu_5Zn_8 nanoparticles, Powder Technol. 318 (2018) 549–557.
[5] S. Grasso, Y. Sakka, G. Maizza, Electric current activated/assisted sintering (ECAS): a review of patents 1906–2008, Sci. Technol. Adv. Mater. 10 (5) (2009), 053001.
[6] M.A. Lagos, I. Agote, T. Schubert, T. Weissgaerber, J.M. Gallardo, J.M. Montes, L. Prakash, C. Andreouli, V. Oikonomou, D. Lopez, J.A. Calero, Development of electric resistance sintering process for the fabrication of hard metals: processing, microstructure and mechanical properties, Int. J. Refract. Met. H 66 (2017) 88–94.
[7] J.M. Montes, F.G. Cuevas, J. Cintas, P. Urban, A one-dimensional model of the electrical resistance sintering process, Metall. Mater. Trans. A 46 (2) (2014) 963–980.
[8] S. Cecchel, D. Ferrario, A. Panvini, G. Cornacchia, Lightweight of a cross beam for commercial vehicles: development, testing and validation, Mater. Des. 149 (2018) 122–134.
[9] C. Chen, C. Lin, In-situ dispersed La oxides of Al6061 composites by mechanical alloying, J. Alloys Compd. 775 (1) (2019) 1156–1163.
[10] V. Sivananth, S. Vijayarangan, N. Rajamanickam, Evaluation of fatigue and impact behavior of titanium carbide reinforced metal matrix composites, Mater. Sci. Eng. A-Struct. 597 (2014) 304–313.
[11] S. Huo, B. Mais, J. Gradl, Pressing characteristics for PM aluminum alloys, in: Advances in Powder Metallurgy and Particulate Materials, vol. 7, MPIF, NJ, USA, 2012, pp. 143–154.
[12] A. Kurzawa, D. Pyka, K. Jamroziak, M. Bocian, P. Kotowski, P. Widomski, Analysis of ballistic resistance of composites based on EN AC-44200 aluminum alloy reinforced with Al_2O_3 particles, Compos. Struct. 201 (2018) 834–844.
[13] J. Oñoro, M.D. Salvador, L.E.G. Cambronero, High-temperature mechanical properties of aluminium alloys reinforced with boron carbide particles, Mater. Sci. Eng. A-Struct. 499 (2009) 421–426.
[14] R. Valiev, Nanostructuring of metals by severe plastic deformation for advanced properties, Nat. Mater. 3 (2004) 511–516.
[15] A.P. Newbery, B. Ahn, T.D. Topping, P.S. Pao, S.R. Nutt, E.J. Lavernia, Large UFG Al alloy plates from cryomilling, J. Mater. Process. Technol. 203 (1–3) (2008) 37–45.
[16] M. Zabihi, M.R. Toroghinejad, A. Shafyei, Application of powder metallurgy and hot rolling processes for manufacturing aluminum/alumina composite strips, Mater. Sci. Eng. A-Struct. 560 (2013) 567–574.
[17] H. Mohseni, S. Keirs, S.L.I. Chan, M. Ferry, High temperature stability of fine grained 7075 Al alloy containing nanosized SiC particles, Mater. Sci. Tech. Lond. 26 (2010) 597–603.
[18] E.S. Caballero, J. Cintas, F.G. Cuevas, J.M. Montes, F. Ternero, Influence of milling atmosphere on the controlled formation of ultrafine dispersoids in Al-based MMCs, Metals 6 (9) (2016) 224–232.
[19] K. Zhao, D. Tang, J.-L. Liu, Y.-G. Wang, Structural evolution during mechanical milling of bimodal-sized Al2O3 particles reinforced aluminum matrix composite, Acta Metall. Sin. (Engl. Lett.) 31 (2018) 423–430.
[20] X. Li, X. Wen, H. Zhao, Z. Ma, L. Yu, C. Li, C. Liu, Q. Guo, Y. Liu, The formation and evolution mechanism of amorphous layer surrounding Nb nano-grains in Nb-Al system during mechanical alloying process, J. Alloys Compd. 779 (2019) 175–182.
[21] MPIF Standard 46, Determination of tap density of metal powders, in: Standard Test Methods for Metal Powders and Powder Metallurgy Products, MPIF, Metal Powder Industries Federation, Princeton, NJ, USA, 2016.
[22] A. Le Bail, Whole powder pattern decomposition methods and applications: a retrospection, Powder Diffr. 20 (4) (2005) 316–326.
[23] F.V. Lenel, Resistance sintering under pressure, JOM 7 (1955) 158–167.
[24] J. Cintas, F.G. Cuevas, J.M. Montes, E.S. Caballero, E.J. Herrera, Strengthening of ultrafine PM aluminium using nano-sized oxycarbonitride dispersoids, Mater. Sci. Eng. A-Struct. 528 (28) (2011) 8286–8291.
[25] U.R. Evans, The Corrosion and Oxidation of Metals: First Supplementary, Edward Arnold, London, UK, 1968.
[26] N. Tsuda, K. Nasu, A. Fujimori, K. Siratori, Electronic Conduction in Oxides, second ed., Springer, New York, USA, 2000.